minerals

MDPI

Article

Study on Hydrometallurgical Treatment of Oxide Ores Bearing Zinc

Jinlin Yang [1,2], Xingnan Huo [1], Zongyu Li [1] and Shaojian Ma [1,2,*]

[1] College of Resources, Environment and Materials, Guangxi University, Nanning 530004, China
[2] Guangxi Key Laboratory of Processing for Nonferrous Metallic and Featured Materials, Guangxi University, Nanning 530004, China
* Correspondence: 1615391004@alu.gxu.edu.cn; Tel.: +86-131-5266-0958

Abstract: As the depletion of zinc sulfide ores becomes more severe, investigations into the recovery of zinc from zinc oxide ores have aroused more interest. In this regard, acid-based hydrometallurgical treatment strategies have had great effectiveness. However, they are inadequate for low-grade zinc oxide ores. In this study, we examined the alkaline treatment of gossan for the recovery of oxide ores that bear zinc, such as siderite and limonite. Additionally, of particular note, the effects of a leaching agent, its concentration and time, temperature, liquid-to-solid ratio, as well as the agitation rate on the leaching of zinc from gossan were studied to evaluate the effects of these parameters on the kinetics of zinc dissolution. The results showed that the leaching of zinc is controlled by a single rate-controlling step with an activation energy of 4.458 kJ/mol before 120 min and 5.536 kJ/mol after 120 min, with zinc leaching efficiency less than 50% in all leachings.

Keywords: gossan; zinc; oxide ore; leaching; alkaline treatment

Citation: Yang, J.; Huo, X.; Li, Z.; Ma, S. Study on Hydrometallurgical Treatment of Oxide Ores Bearing Zinc. *Minerals* **2022**, *12*, 1264. https://doi.org/10.3390/min12101264

Academic Editor: Kyoungkeun Yoo

Received: 17 September 2022
Accepted: 6 October 2022
Published: 7 October 2022

1. Introduction

Gossan is a massive deposit formed by the oxidation and weathering of sulfide deposits. Its composition is dominated by neo-formed minerals, mainly oxidate, secondary sulfates, vitriol-bearing iron, and manganese such as goethite and hematite derived from sulfide oxidation. Gossan also contains remnants of gangue minerals, generally primary clays such as silicates bearing silicon, aluminum, and calcium [1–8].

Many metals such as lead, zinc, copper, nickel, and cobalt dissolve in sulfuric acid, and sulfuric acid is formed by the oxidation of pyrite and other sulfides as the sulfides weather and leach. These metals can then either co-precipitate with Fe compounds or adsorb onto their surfaces. The initial product of weathering is mainly amorphous ferric hydroxide, $Fe(OH)_3$, which gradually crystallizes to either goethite or hematite. Other important minerals associated with Fe oxides include jarosite, gypsum, clay minerals, and silica. If the metal and Fe compounds co-precipitate, they are incorporated into the Fe-mineral structure via isomorphous substitution, thus causing distortions in the unit cell dimensions depending on the ionic radii differences. During the weathering of sulfide minerals, silver, lead, and copper are strongly adsorbed by iron oxides under acidic conditions. In addition, gold can also form stable thiosulfate complexes that are oxidized into sulfates in sulfide-rich ore deposits under higher oxidation conditions. Therefore, gold remains in the iron cap as the main residual mineral and can be recovered [9–12].

Zinc mainly comes from zinc sulfide ores, as sulfides are easy to be separated from gangue and can be enriched by conventional flotation techniques. However, with the continuous depletion of sulfide ores, strategies for extracting zinc metal from oxidized zinc ores are also being explored. Such ores include zinc-bearing minerals such as smithsonite ($ZnCO_3$), hydrozincite ($2ZnCO_3{\cdot}3Zn(OH)_2$), zincite (ZnO), willemite (Zn_2SiO_4), hemimorphite ($Zn_4Si_2O_7(OH)_2{\cdot}H_2O$), and other oxide minerals such as siderite ($FeCO_3$) and limonite ($FeOOH{\cdot}nH_2O$). Additionally, zinc oxide ores are usually difficult to separate.

In many reports on the recovery of zinc oxide ores, at least two approaches for their processing have been identified. Firstly, zinc oxide ores are concentrated by conventional physical separation methods such as flotation, gravity separation, or magnetic separation, with low metal recovery and high operating costs [13–16]. Secondly, zinc oxide ores can be treated via pyrometallurgical or hydrometallurgical methods. However, in actual practice, the pyrometallurgical process is not that ideal because of its heavy pollution, large energy consumption, and heavy capital investment [17,18]. Thus, various types of hydrometallurgical processes have been developed, i.e., the acidic leaching process, which has been widely applied with good recoveries [19–21]. However, it is becoming increasingly apparent that this process is not economical for low-grade zinc oxide ores with high contents of Fe, Ca, Mg, and SiO_2. In fact, such metals dissolve during the dissolution of zinc minerals, resulting in high acid consumption and complex purification processes [22–24]. To overcome these shortcomings, many studies have explored the alkaline treatment of low-grade zinc oxide ores because iron does not dissolve and silica gel does not form during the leaching process. Consequently, alkaline leaching has become an effective way to process low-grade complex zinc oxide ore with the advantages of low corrosion and low pollution. Alkaline leaching reagents include ammonia, sodium hydroxide, ammonia–ammonium chloride, ammonia–ammonium carbonate, and ammonia–ammonium sulfate. Although many studies concerning the leaching of zincite, smithsonite, willemite, and hemimorphite have been reported, there are still no reports on the recovery of oxide ores bearing zinc, such as siderite and limonite, from gossan using alkaline treatment. To this end, the purpose of this research was to study the leaching of zinc from siderite and limonite using alkaline solution and to assess the effects of several experimental conditions on the kinetics of zinc dissolution.

2. Materials and Methods

2.1. Elemental Analysis

Samples used in this study were obtained from Guangxi Zhuang Autonomous Region, China. X-fluorescence analysis was used, and the results of the semi-quantitative analysis of the samples with multiple elements are shown in Table 1. It can be seen that the composition of chemical elements of the sample is simple; the main chemical elements are Fe, Zn, Si, Al and O, and the content of other elements is small.

Table 1. Chemical components of Tongkeng ore.

Component	Zn	Fe	SiO_2	Al_2O_3	CaO	MgO	S	Pb	Mn	Cd
Content/%	13	40.2	5.9	4.5	0.8	0.3	0.36	0.1	0.09	0.02

2.2. XRD Analysis

The X-ray diffraction data shown in Figure 1 indicate that the main zinc-bearing minerals are smithsonite, siderite, and limonite, and the gangue mineral is quartz. Additionally, by analyzing the mineral types and occurrences, the distributions of zinc in these minerals were determined. As can be seen from Table 2, the main minerals bearing zinc are siderite and limonite. Therefore, it can be inferred that zinc exists in gossan ores in the forms of siderite, limonite, and smithsonite.

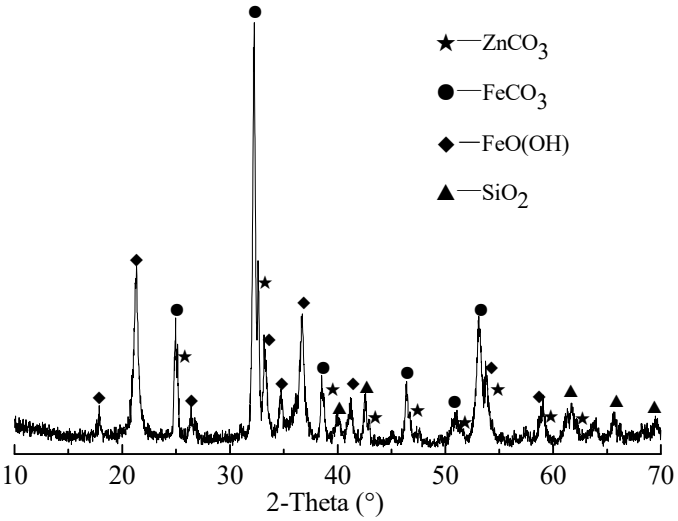

Figure 1. XRD pattern of the raw ore.

Table 2. Distribution of zinc in the main minerals of the raw ore sample.

Minerals	Mineral Content/%	Zinc Content/%	Zinc Distribution Rate/%
Siderite bearing zinc	41.87	10.53	33.93
Smithsonite	2.58	52.06	10.33
Limonite bearing zinc	51.93	13.85	55.35
Gangue	3.62	1.40	0.39
Total	100.00	13.00	100.00

2.3. Leaching Rate Calculation

Metal leaching velocity η has been used as an index to assess the leaching effect.

The leaching rate of zinc can be calculated by weighing the leaching residue and analyzing the zinc content of the leaching residue. The formula to calculate is as follows:

$$\eta_{Zn} = \frac{(M\alpha_{Zn} - m\theta_{Zn})}{M\alpha_{Zn}} \times 100$$

where η_{Zn} is the leaching rate of zinc, %; M is the mass of sample before leaching, g; α_{Zn} is the zinc grade in the sample, %; m is the mass of leached slag, g; θ_{Zn} is the zinc grade in the leached slag, %.

2.4. Modeling of Dynamics

Dynamics modeling tasks mainly include two aspects: one is contraction of the reaction core model and the class model choice and judgment; the second, according to the results of test data, the mathematical model for fitting. The main application of the kinetic model is to calculate the activation energy of each reaction process or stage according to the relation equation of velocity constant and temperature established by Arrhenius and judge the type of control steps of the reaction accordingly.

2.5. Leaching Experiments

Ammonia, ammonia–ammonium carbonate, sodium hydroxide, ammonia–ammonium sulfate, and ammonia–ammonium chloride were used as the leaching reagents in the leaching and kinetic experiments. Leaching tests were carried out in a flask on a thermostatically controlled magnetic stirrer. Then, 50 g of ore was added to an agitated leaching solution with a known amount of alkaline solution and maintained at a required temperature. The liquid-to-solid ratio was kept constant. Parameters such as the leaching reagent, alkaline concentration, leaching time and temperature, L/S ratio, as well as agitation rate were

studied. The optimum leaching conditions were determined according to the following steps: 50 g of the sample was leached with alkaline solutions of different concentrations and stirred with a magnetic stirrer at a rotational speed of 400 rpm. To determine the effect of leaching time, 50 g of the sample was leached in a known alkaline solution at 60 °C at different intervals with an L/S ratio of 4:1. To determine the effect of leaching temperature, the leaching temperature varied while all other parameters remained fixed. Finally, the optimal L/S ratio was determined using a 4 mol·L^{-1} alkaline solution with the required concentration in the solid sample at 60 °C and 120 min. From the above experiments, the overall optimum leaching conditions were determined.

3. Results and Discussion

3.1. Effects of Various Leaching Conditions

3.1.1. Effect of Leaching Agent

Figure 2 shows the correlation between the zinc leaching efficiency and leaching time with different leaching agents. The results showed that the leaching rate of zinc increased greatly with the increase in leaching time from 10 min to 120 min. However, after 120 min, the leaching rate was significantly reduced. Overall, the zinc leaching efficiency was below 50%, which may have been caused by the different origins and properties of the gossan ore minerals. Figure 2 also shows that the leaching efficiency of gossan ore leached by ammonia–ammonium chloride was higher than that of other leaching agents. The reason for this may have been that the electrostatic interactions between zinc and this leaching reagent were stronger than those of the other leaching agents.

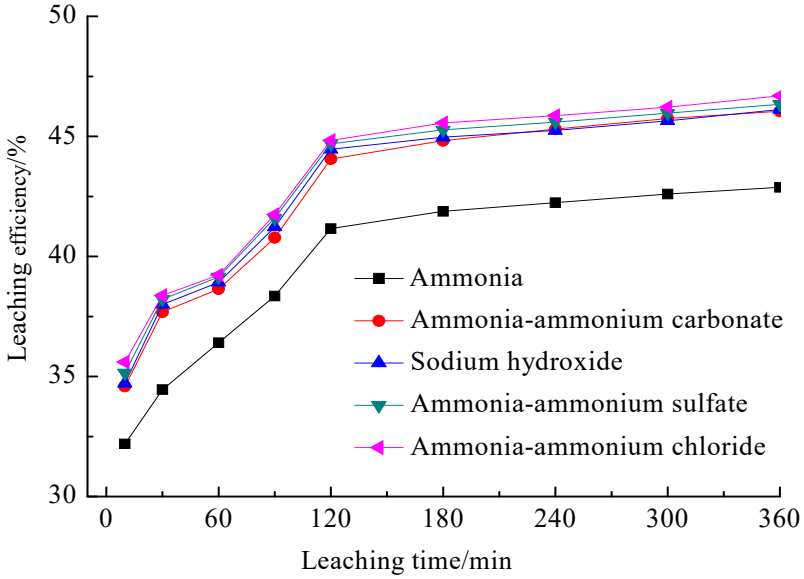

Figure 2. Effect of leaching time on the leaching efficiency of zinc in different lixiviants.

As noted in Section 2.1, zinc exists in the gossan ores in the form of siderite, limonite, and smithsonite. The present results suggest that zinc in smithsonite can be dissolved in the leaching solution, whereas zinc in limonite can be partly desorbed under external forces. Zinc in siderite cannot be recovered due to its solubility in the leaching agent. Therefore, it can be concluded that it is difficult to recover zinc from gossan ore via this alkaline leaching method.

Figure 3 shows the XRD patterns of the leaching slags after different lixiviant leaching. Compared with the XRD pattern of the raw ore (Figure 1), the diffraction peaks of smithsonite in the samples leached by different lixiviants decreased, indicating that smithsonite was leached by alkaline solutions. Based on the zinc content and slag properties, the main forms of residual zinc are isomorphism and adsorption in siderite and limonite, respectively.

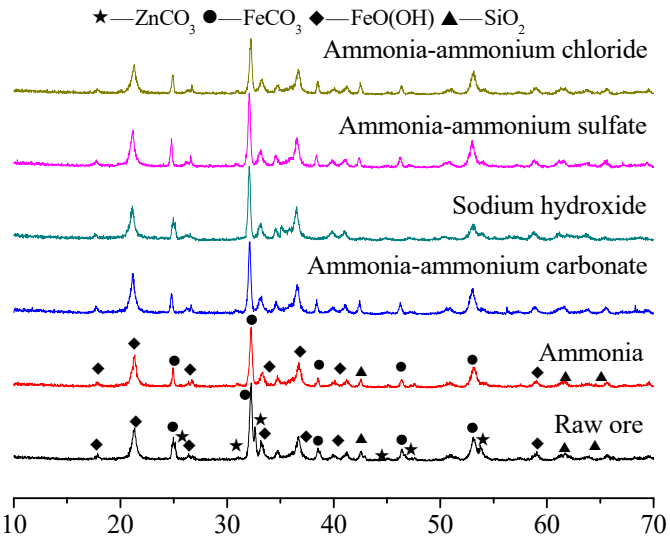

Figure 3. XRD patterns of the leaching products by different lixiviants.

3.1.2. Effect of Leaching Agent Concentration

Ammonia–ammonium chloride was used as the leaching agent here and in the subsequent tests. In all kinds of investigation cases, the initial leaching agent concentration was varied at first, while other parameters were kept constant: the leaching time (120 min), leaching temperature (60 °C), L/S ratio (4:1), and agitation rate (400 rpm). Figure 4 shows the correlation between zinc leaching efficiency and leaching agent concentration under these conditions. The results demonstrate that when the ammonia–ammonium chloride concentration increased from 2 mol·L^{-1} to 4 mol·L^{-1}, the metal leaching efficiency was significantly improved. However, the leaching efficiency of zinc varied slightly after 4 mol·L^{-1}.

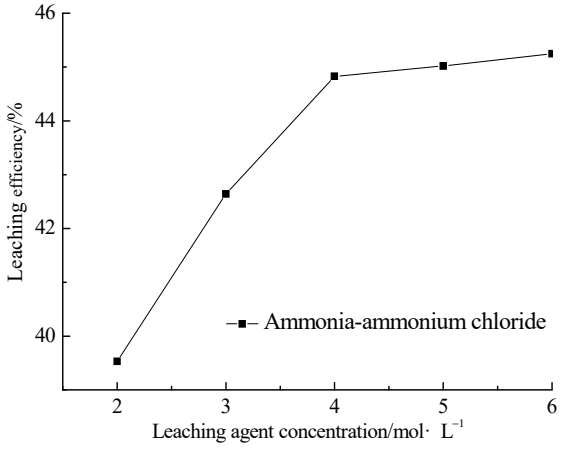

Figure 4. Effect of leaching agent concentration on zinc extraction.

3.1.3. Effect of Leaching Time

As metal extraction can be improved by prolonged leaching times, the leaching time duration was varied to examine its influence on zinc leaching efficiency. Specifically, the leaching tests were performed as the leaching time varied from 10 min to 360 min and the leaching temperature was 60 °C. The values of leaching agent concentration, L/S ratio, and agitation rate were maintained at 4 mol·L^{-1}, 4:1, and 400 rpm, respectively. Figure 5 shows the variation in the leaching efficiency of zinc as a function of leaching time at 60 °C. The zinc leaching efficiency also increased with leaching time. Yet, the zinc leaching efficiency only increased rapidly before the leaching time reached 120 min, and after that, the efficiency changes became relatively small.

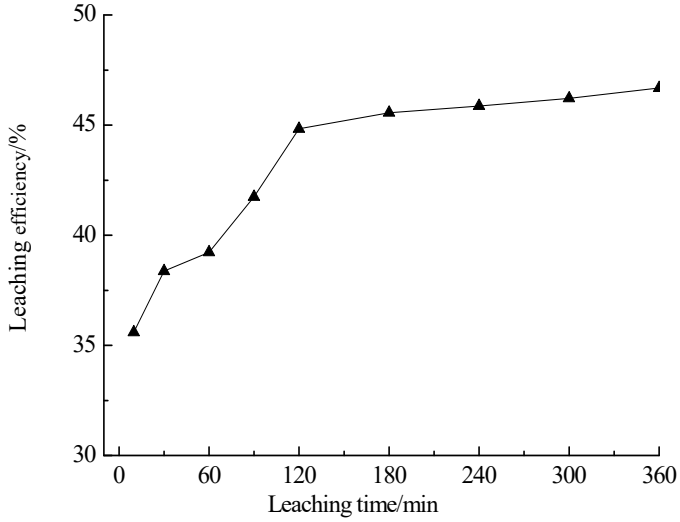

Figure 5. Effect of leaching time on zinc extraction.

3.1.4. Effect of Leaching Temperature

Leaching temperature varied from 30 °C to 90 °C in the leaching tests; the alkaline concentration range was 4 mol·L^{-1}; and the leaching time, L/S ratio, and agitation rate remained constant at 120 min, 4:1, and 400 rpm, respectively. The effects of temperature on the efficiency of zinc extraction are plotted in Figure 6. The zinc leaching efficiency rose from 36.29% to 46.34% with the increase in temperature. Obviously, the reaction temperature exerted no significant impact on the leaching efficiency of zinc.

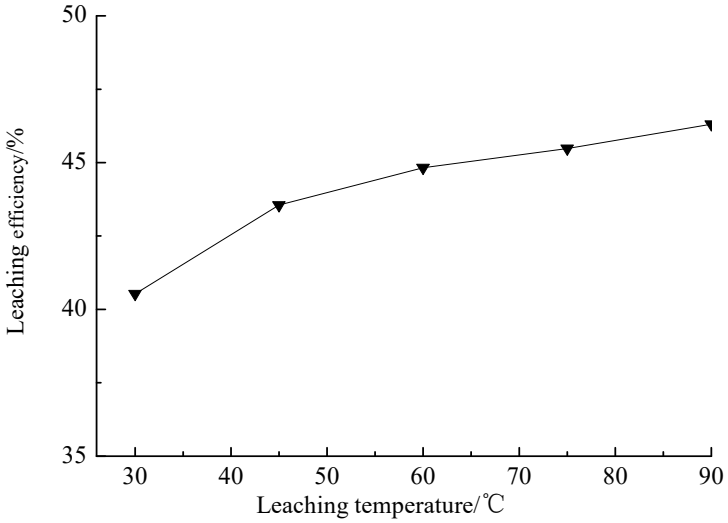

Figure 6. Effect of leaching temperature on zinc extraction.

3.1.5. Effect of L/S Ratio

The effect of the liquid-to-solid ratio on the extraction of zinc was investigated with six different L/S ratios. For these tests, the alkaline concentration, leaching temperature, leaching time, and agitation rate were maintained at 4 mol·L^{-1}, 60 °C, 120 min, and 400 rpm, respectively. Figure 7 shows the variation in zinc leaching efficiency as a function of the L/S ratio under the above conditions. As can be seen from the figure, when the L/S ratio was greater than 4:1, the extraction rate of zinc did not change significantly.

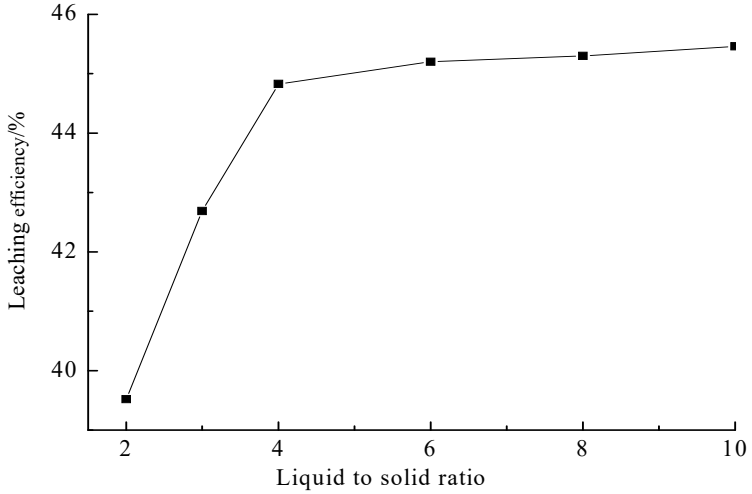

Figure 7. Effect of L/S on zinc extraction.

3.1.6. Effect of Agitation Rate

The leaching efficiency of zinc can be improved by increasing the agitation rate as it keeps mineral particles suspended in the liquor and reduces the thickness of the mass transfer boundary layer on the particle surface. For these reasons, the effect of the agitation rate on the leaching efficiency of zinc was examined. The leaching tests were carried out with the agitation rate varying from 200 rpm to 600 rpm. For these tests, the leaching agent concentration, leaching time, leaching temperature, and L/S ratio were maintained at 4 mol·L^{-1}, 120 min, 60 °C, and 4:1, respectively. Figure 8 shows the variation in the leaching efficiency of zinc as a function of the agitation rate. The efficiency of zinc leaching was obviously improved when the agitation rate rose from 200 rpm to 400 rpm. After 400 rpm, however, the leaching efficiency remained almost unchanged. Therefore, zinc extraction efficiency is optimal at 400 rpm, and higher agitation has no obvious benefit in terms of its associated increased capital and operating costs.

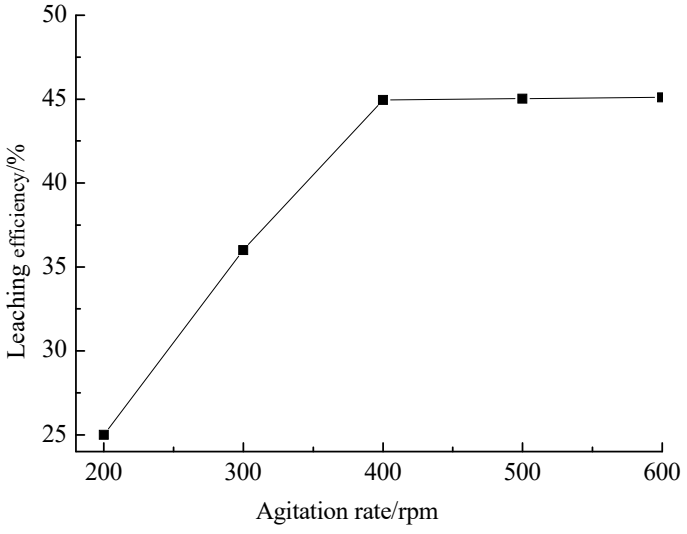

Figure 8. Effect of agitation rate on zinc extraction.

3.2. Kinetic Analysis

In a fluid–solid reaction system, the reaction rate is generally controlled by one of the following steps: diffusion through the fluid membrane, diffusion through the product

layer, or a chemical reaction of unreacted particles on the core surface. Zinc oxide and zinc carbonate react with ammonia–ammonium chloride according to the following reactions:

$$ZnCO_3 + 2NH_4^+ + 2NH_3 \rightarrow Zn(NH_3)_4^{2+} + H_2O + CO_2, \quad (1)$$

$$ZnO + 2NH_4^+ + 2NH_3 \rightarrow Zn(NH_3)_4^{2+} + H_2O, \quad (2)$$

Clearly, as the reaction progresses, the size of the initial particle decreases. Thus, the shrinking core model with variable particle sizes can be used to describe these reactions. This process can be simulated by an isometric spherical particle of changing size with a surface reaction or diffusion-controlled regime. If the process is controlled by the diffusion resistance of fluid film, the reaction fraction of zinc at any time can be calculated based on the following equation, which is applicable to small particles moving in the Stokes regime:

$$1 - (1 - x)^{\frac{2}{3}} = \frac{t}{t_f}, \quad (3)$$

where x is the fraction of reacted zinc. The time for the complete disappearance of a particle, s, can be calculated from:

$$t_f = \frac{\rho R_S}{bMk_g c_A}, \quad (4)$$

$$t = \frac{\rho R_S}{bMk_g c_A}\left[1 - (1 - x)^{\frac{2}{3}}\right], \quad (5)$$

ρ stands for the density of the solid reactant, Rs the radius of the unreacted particle, b the stoichiometric coefficient of the reaction, M the relative molecular mass of the solid reactant, k_g the mass transfer coefficient, and c_A the leaching agent concentration.

In order to determine the kinetic parameters and rate-controlling steps of zinc leaching in an ammonia–ammonium chloride solution, the experimental data were analyzed on the basis of the shrinking core model (Equation (5)). The validity of the experimental data to the integral rate was tested using statistical and graphical methods, and multiple regression coefficients obtained for the integral rate expression were calculated. The calculated regression coefficients indicate that this method is most suitable for the rate expression of fluid film diffusion control. Similarly, from the results of the statistical analysis, the leaching of zinc from gossan in ammonia–ammonium chloride solutions was found to be controlled by fluid film diffusion. The corresponding integral rate expression was determined to obey the following rate equation:

$$1 - (1 - x)^{\frac{2}{3}} = kt, \quad (6)$$

$$k = \left(k_0 e^{-\frac{E_0}{RT}}\right) \times t \quad (7)$$

Equation (6) provides the best straight lines relative to the other equations tested. Plots of $1 - (1 - x)^{2/3}$ versus t are shown in Figure 9 (before 120 min) and after 120 min is shown in Figure 10 at various reaction temperatures with a specific range of particle sizes and leaching agent concentration under a given L/S ratio. The apparent rate constants, k, were evaluated by the corresponding slopes of the straight lines. Using the Arrhenius equation (Equation (7)), a plot of ln$k$ versus $1/T$ should give a straight line with slope $-E_0/RT$ and intercept lnk_0. To this end, the experimental data were combined with Equation (7) to draw ln$k$ versus $1/T$ for each value of the reaction temperature. Figure 11 shows 120 min ago. After 120 min, is shown in Figure 12. In this way, the activation energies (E_0) and reaction rates (k_0) with leaching times before and after 120 min were calculated as 4.458 kJ·mol^{-1} and 4.22×10^2 and 5.536 kJ·mol^{-1} and 2.84×10^3, respectively.

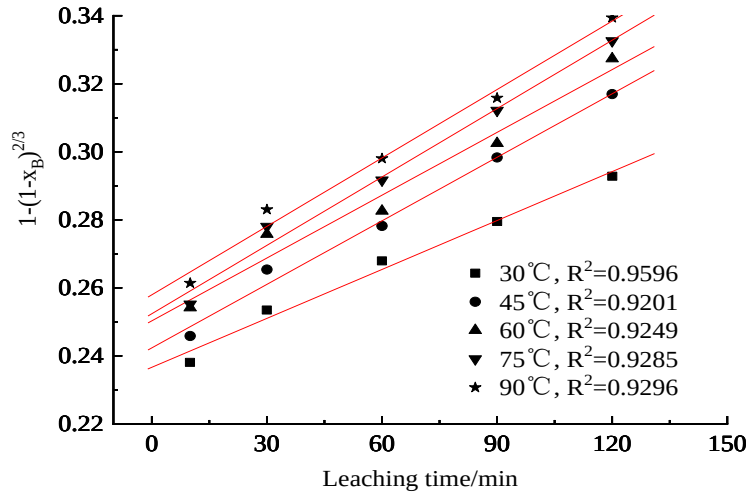

Figure 9. Relation of $1-(1-x)^{2/3}$ and leaching time at different temperatures for leaching times less than 120 min.

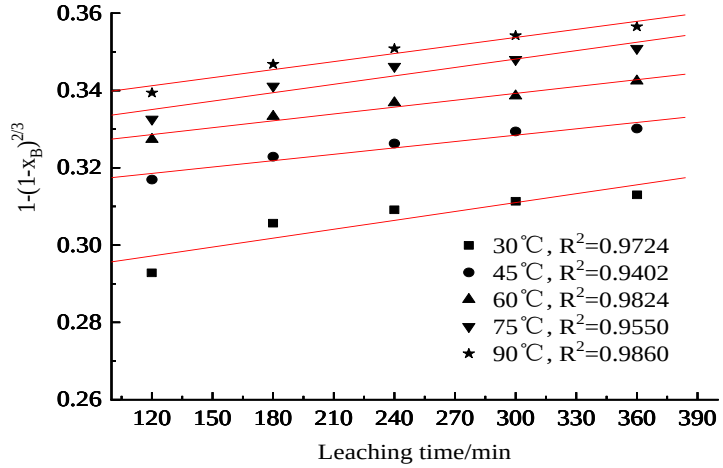

Figure 10. Relation of $1-(1-x)^{2/3}$ and leaching time at different temperatures for leaching times greater than 120 min.

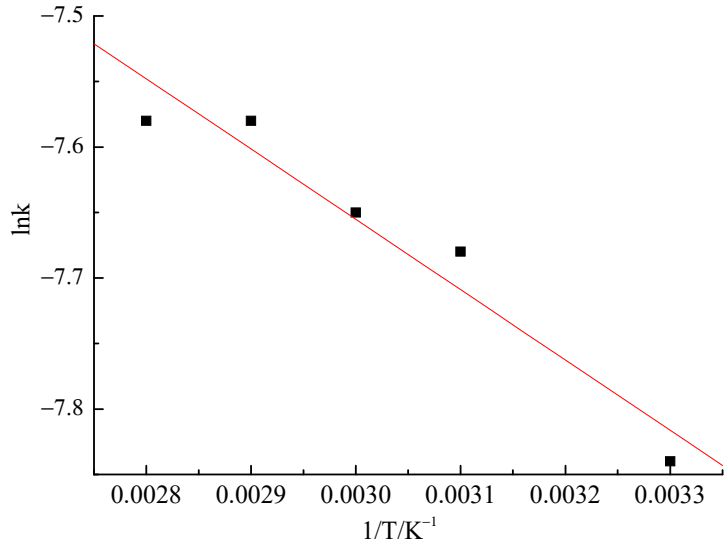

Figure 11. Relation of ln$k$ and $1/T$ (R^2 = 0.9358) for leaching times less than 120 min.

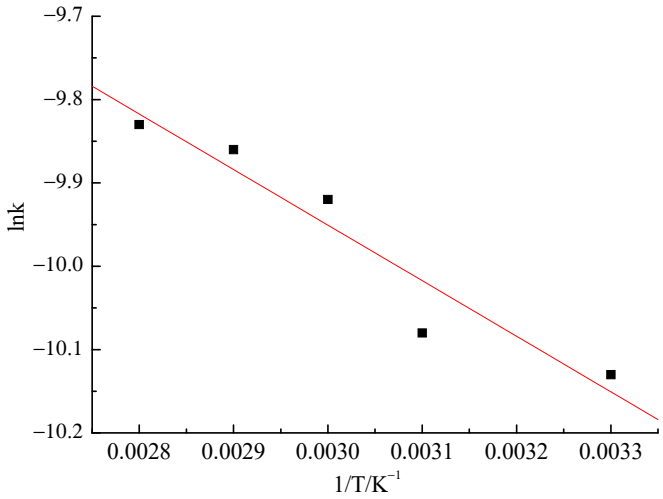

Figure 12. Relation of ln$k$ and $1/T$ (R^2 = 0.9159) for leaching times greater than 120 min.

The values of the activation energy indicate that the process is a fluid film diffusion-controlled process, which is consistent with the research results of similar fluid–solid reaction systems. The value of the activation energy in the dissolution process can help predict the rate-controlling step. That is to say, the activation energy of a diffusion-controlled process typically ranges from 4 to 12 kJ·mol^{-1}, while it is usually greater than 40 kJ mol^{-1} for a chemically controlled process. The relatively small values of the activation energy obtained for the dissolution process indicate that the leaching of zinc from gossan in ammonia–ammonium chloride is controlled by fluid film diffusion. Thus, Equation (6) can be written as follows:

Before 120 min:

$$1 - (1 - x)^{\frac{2}{3}} = \left(4.22 \times 10^2 e^{-\frac{4.458}{RT}}\right) \times t \quad (8)$$

After 120 min:

$$1 - (1 - x)^{\frac{2}{3}} = \left(2.84 \times 10^3 e^{-\frac{5.536}{RT}}\right) \times t \quad (9)$$

Obviously, the activation energy differs before and after 120 min of leaching time. As mentioned in Section 3.1.1, the zinc in smithsonite could be dissolved in the leaching solution, whereas zinc on limonite could be partly desorbed, and zinc in siderite could not be recovered due to its solubility in the leaching agent. The dissolution of zinc in smithsonite occurs quickly, whereas zinc desorption in limonite is relatively slow, which is the key step for alkaline leaching.

4. Conclusions

In summary, the ore used in this study from the gossan of sulfide deposits displayed a complex nature, as evidenced by the chemical analysis. An alkaline leaching method was investigated for its ability to leach zinc from siderite and limonite. The results showed that the leaching efficiency of zinc is 50% lower than that of conventional leaching. By the comparison of the XRD pattern of the raw ore, different diffraction peaks of smithsonite were observed, indicating the successful extraction of smithsonite by the alkaline treatment. Finally, the kinetic analysis of the experimental data indicates that the leaching of zinc from gossan using ammonia–ammonium chloride as the leaching agent is controlled by fluid film diffusion. The activation energy was found to be 4.458 kJ·mol^{-1} for leaching times below 120 min and 5.536 kJ·mol^{-1} above 120 min, which is consistent with a fluid film diffusion-controlled reaction. As well as the fact that alkaline leaching is simple in its process, the raw material is widely available, it has low energy consumption, low cost, and the characteristics of the pollution of the environment's light, there are obvious economic benefits and social benefits. From the above research conclusion, the zinc leaching efficiency

less than 50%. Using the alkali leaching method, it is difficult to recover zinc from iron cap ore, and thus, it cannot be applied to large-scale industrial production.

Author Contributions: Conceptualization, J.Y. and S.M.; data curation, J.Y. and X.H.; formal analysis, X.H. and Z.L.; funding acquisition, J.Y.; investigation, X.H. and Z.L.; methodology, J.Y. and S.M.; project administration, J.Y. and S.M.; validation, X.H. and Z.L.; writing—original draft, J.Y.; writing—review and editing, J.Y. and S.M. All authors have read and agreed to the published version of the manuscript.

Funding: This research was funded by the National Natural Science Foundation of China (No. 52264020, No. 51774099).

Institutional Review Board Statement: Not applicable.

Informed Consent Statement: Not applicable.

Data Availability Statement: Not applicable.

Conflicts of Interest: The authors declare no conflict of interest.

References

1. Belogub, E.V.; Novoselov, C.A.; Spiro, B.; Yakovleva, B.A. Mineralogical and s isotopic features of the supergene profile of the zapadno-ozernoe massive sulphide and au-bearing gossan deposit, South Urals. *Mineral. Mag.* **2016**, *67*, 339–354. [CrossRef]
2. Symons, D.T.A.; Lewchuk, M.T.; Boyle, D.R. Pliocene–pleistocene genesis for the Murray brook and heath steele Au–Ag gossan ore deposits, New Brunswick, from paleomagnetism. *Can. J. Earth Sci.* **2011**, *33*, 1–11. [CrossRef]
3. Santos, E.S.; Abreau, M.M.; de Varennes, A.; Macías, F.; Leitão, S. Evaluation of chemical parameters and ecotoxicity of a soil developed on gossan following application of polyacrylates and growth of *Spergularia purpurea*. *Sci. Total Environ.* **2013**, *461*, 360–370. [CrossRef] [PubMed]
4. Gossan, N.C.; Zhang, F.; Guo, B.; Jin, D.; Yoshitane, H.; Yao, A.; Glossop, N.; Zhang, Y.Q.; Fukada, Y.; Meng, Q.-J. The e3 ubiquitin ligase ube3a is an integral component of the molecular circadian clock through regulating the bmal1 transcription factor. *Nucleic Acids Res.* **2014**, *1048*, 5765–5775. [CrossRef]
5. Dudek, M.; Gossan, N.; Yang, N.; Im, H.-J.; Ruckshanthi, J.P.D.; Yoshitane, H.; Li, X.; Jin, D.; Wang, P.; Boudiffa, M.; et al. The chondrocyte clock gene bmal1 controls cartilage homeostasis and integrity. *J. Clin. Investig.* **2015**, *126*, 365–376. [CrossRef]
6. Gossan, D.P.A.; Magid, A.A.; Kouassi-Yao, P.A.; Behr, J.-B.; Ahibo, A.C.; Djakouré, L.A.; Harakat, D.; Voutquenne-Nazabadioko, L. Glycosidase inhibitors from the roots of *Glyphaea brevis*. *Phytochemistry* **2014**, *109*, 76–83. [CrossRef]
7. Atapour, H.; Aftabi, A. The geochemistry of gossans associated with *Sarcheshmeh porphyry* copper deposit, Rafsanjan, Kerman, Iran: Implications for exploration and the environment. *J. Geochem. Explor.* **2007**, *93*, 47–65. [CrossRef]
8. Baggio, S.B.; Hartmann, L.A.; Massonne, H.J.; Theye, T.; Antune, L.M. Silica gossan as a prospective guide for amethyst geode deposits in the Ametista do Sul mining district, Paraná volcanic province, southern Brazil. *J. Geochem. Explor.* **2015**, *159*, 213–226. [CrossRef]
9. Safari, V.; Arzpeyma, G.; Rashchi, F.; Mostoufi, N. A shrinking particle-shrinking core model for leaching of a zinc ore containing silica. *Int. J. Miner. Process.* **2009**, *93*, 79–83. [CrossRef]
10. Espiari, S.; Rashchi, F.; Sadrnezhaad, S.K. Hydrometallurgical treatment of tailings with high zinc content. *Hydrometallurgy* **2006**, *82*, 54–62. [CrossRef]
11. Qin, W.Q.; Li, W.Z.; Lan, Z.Y.; Qiu, G.Z. Simulated small-scale pilot plant heap leaching of low-grade oxide. *Miner. Eng.* **2007**, *8*, 694–700. [CrossRef]
12. Chen, A.L.; Zhao, Z.W.; Jia, X.J.; Long, S.; Huo, G.S.; Chen, X.Y. Alkaline leaching Zn and its concomitant metals from refractory hemimorphite zinc oxide ore. *Hydrometallurgy* **2009**, *97*, 228–232. [CrossRef]
13. Li, S.L.; Ma, X.M.; Wang, J.C.; Xing, Y.W.; Gui, X.H.; Cao, Y.J. Effect of polyethylene oxide on flotation of molybdenite fines. *Miner. Eng.* **2020**, *146*, 106–146. [CrossRef]
14. Luo, B.; Liu, Q.J.; Deng, J.H.; Yu, L.; Lai, H.; Song, C.; Li, S.M. Characterization of sulfide film on smithsonite surface during sulfidation processing and its response to flotation performance. *Powder Technol.* **2019**, *351*, 144–152. [CrossRef]
15. Lei, C.; Yan, B.; Chen, T.; Xiao, X.M. Recovery of metals from the roasted lead-zinc tailings by magnetizing roasting followed by magnetic separation. *J. Clean. Prod.* **2017**, *1581*, 73–80. [CrossRef]
16. Pluokun, O.O.; Otunniyi, I.O. Chemical conditioning for wet magnetic separation of printed circuit board dust using octyl phenol ethoxylate. *Sep. Purif. Technol.* **2020**, *2401*, 116586. [CrossRef]
17. Gnoinski, J. Skorpion zinc: Optimization and innovation. *J. S. Afr. Inst. Min. Metall.* **2007**, *107*, 657–662.
18. De Wet, J.R.; Singleton, J.D. Development of a viable process for the recovery of zinc from oxide ores. *J. S. Afr. Inst. Min. Metall.* **2008**, *108*, 253–259.
19. Feng, L.Y.; Yang, X.W. Pelletizing and alkaline leaching of powdery lowgrade zinc oxide ores. *Hydrometallurgy* **2007**, *89*, 305–310. [CrossRef]

20. Sole, K.C.; Feather, A.M.; Cole, P.M. Solvent extraction in southern Africa: An update of some recent hydrometallurgical developments. *Hydrometallurgy* **2005**, *78*, 52–78. [CrossRef]
21. Ashraf, M.; Zafar, Z.I.; Ansari, T.M. Selective leaching kinetics and upgrading of low-grade calcareous phosphate rock in succinic acid. *Hydrometallurgy* **2015**, *80*, 286–292. [CrossRef]
22. Yuan, S.; Zhou, W.T.; Han, Y.X.; Li, Y.J. Efficient enrichment of low grade refractory rhodochrosite by preconcentration-neutral suspension roasting-magnetic separation process. *Powder Technol.* **2020**, *361*, 529–539. [CrossRef]
23. Demir, F.; Dönmez, B.; Çolak, S. Leaching kinetics of magnesite in citric acid solution. *J. Chem. Eng. Jpn.* **2003**, *36*, 683–688. [CrossRef]
24. Laçin, O.; Dönmez, B.; Demir, F. Dissolution kinetics of natural magnesite in acetic acid solutions. *Int. J. Miner. Process.* **2005**, *75*, 91–99. [CrossRef]